Kinetics of Association and Dissociation of Two Enantiomers, NSC 613863 (*R*)-(+) and NSC 613862 (*S*)-(−) (CI 980), to Tubulin[†]

Pascale Barbier,[‡] Vincent Peyrot,*[,‡] Chantal Dumortier,[§] An D'Hoore,[§] Gregory A. Rener,[∥] and Yves Engelborghs[§]

Proteines et Cancer, URA−CNRS 1924, Faculté de Pharmacie, 27 Boulevard Jean Moulin, F-13385 Marseille Cedex 5, France, Laboratory of Chemical and Biological Dynamics, Katholieke Universiteit Leuven, Celestijnenlaan 200 D, B-3001 Leuven, Belgium, and Kettering-Meyer Laboratory, Southern Research Institute, P.O. Box 55305, Birmingham, Alabama

Received August 21, 1995; Revised Manuscript Received November 16, 1995[⊗]

ABSTRACT: The kinetics of binding of R- and S-enantiomers were studied by the fluorescence stopped-flow technique. For the R-enantiomer, the time course of the increase in fluorescence is best fitted by a sum of two exponentials. In pseudo-first-order conditions, the first observed rate constant showed a linear concentration dependence whereas the second showed a hyperbolic one. The dissociation rate constants were determined independently by displacement experiments with 2-methoxy-5-(2,3,4-trimethoxyphenyl)-2,4,6-cycloheptatrien-1-one (MTC). The two exponential phases were assumed to be due to a two-step binding mechanism: an initial binding followed by a conformational change. This is different from colchicine and MTC binding, where the two phases show a hyperbolic concentration dependence and are attributed to the parallel binding to different isoforms of tubulin [Banerjee, A., & Luduena, R. F. (1992) *J. Biol. Chem. 267,* 13335−13339]. R-isomer binding did not discriminate between the tubulin isoforms. The temperature dependence of all the rate constants were measured, and the entire thermodynamic reaction path was constructed. For the S-isomer, the direct fluorescence stopped-flow study showed that the signals were largely imputable to the fluorescence of the binding at low-affinity sites [Leynadier, D., Peyrot, V., Sarrazin, M., Briand, C., Andreu, J. M., Rener, G. A., & Temple, C., Jr. (1993) *Biochemistry 32,* 10674−10682]. Therefore, we exploited the competition between R- and S-isomers to determine the binding kinetics of the S-isomer to the R-site. The observed rate constants for competitive binding showed a linear concentration dependence, thus allowing us to calculate the association rate constant of the S-isomer to the R-site. The kinetics of displacement of the S-isomer by MTC allowed the dissociation rate constant for the S-isomer to be determined. The binding of both enantiomers to tubulin in presence of tropolone methyl ether (analog of the colchicine C ring) was decreased, indicating the involvement of the C subsite.

Microtubules participate in a wide variety of cellular functions such as motility, intracellular transport, generation and maintenance of cell shape, sensory transduction, and, especially, mitosis (Olmsted & Borisy, 1973; Dustin, 1984). The major constituent of a microtubule is a heterodimeric protein called tubulin (Luduena, 1977), which is the target of numerous antimitotic drugs.

The best known group of such molecules is that of colchicine (Figure 1) and its analogs, which have been studied in great detail. Stopped-flow kinetic studies of colchicine binding (Garland, 1978; Lambeir & Engelborghs, 1981) showed that the binding process includes two exponential phases which have a nonlinear concentration dependence due to the presence of two steps: a fast initial binding of relatively low affinity followed by a rather slow conformational change of the initial complex. Banerjee and Luduena (1987) reported that β_{III} isotype-depleted tubulin binds colchicine in a monophasic manner, with the disappearance of the slow phase. Later, they showed that adding the purified β_{III} isotype to β_{III}-depleted tubulin restored the biphasic kinetic behavior (Banerjee & Luduena, 1991). Recently, kinetic studies of the interaction of colchicine with pure preparations of $\alpha\beta_{II}$, $\alpha\beta_{III}$, and $\alpha\beta_{IV}$ tubulin dimers confirmed their initial work: the two parallel phases correspond to the presence of two major tubulin isoforms (Banerjee & Luduena, 1992).

MTC[1] (Figure 1), a bifunctional analog of colchicine but without the middle ring, also binds to tubulin in two steps but with some differences in the thermodynamic parameters, as compared with colchicine (Engelborghs & Fitzgerald, 1986, 1987). The kinetic study of the binding of MDL 27048 (Figure 1), which has a slightly different methoxybenzene ring (A), also revealed a two-step binding process on different isoforms of tubulin (Silence *et al*., 1992), which differ in their kinetic constants and the energy parameters. Recently, kinetic studies of several analogs of the middle ring of colchicine have shown that this ring is responsible for the energy barrier of the binding, which largely depends on the electronic nature of the substituent in C_7 position (Pyles & Hastie, 1993).

[†] This research was supported by grants from ARC (Association pour la Recherche contre le Cancer) and la Federation des centres de lutte contre le Cancer and by the program for scientific exchange between the Flemish Community and France (Tournesol T.92.4). A.D'H. and C.D. were supported by IWONL/IWT (Belgium).

* To whom correspondence should be addressed.

[‡] URA-CNRS, 1924.

[§] Katholieke Universiteit Leuven.

[∥] Kettering-Meyer Laboratory.

[⊗] Abstract published in *Advance ACS Abstracts,* January 1, 1996.

[1] Abbreviations: DMSO, dimethyl sulfoxide; SDS, sodium dodecyl sulfate; GTP, guanosine 5′-triphosphate; EGTA, ethylene glycol-bis-(*β*-aminoethyl ether) *N,N,N′,N′*-tetraacetic acid; MES, 2-(*N*-morpholino)ethanesulfonic acid; MDL 27048, *trans*-1-(2,5-dimethoxyphenyl)-3-[4-(dimethylamino)phenyl]-2-methyl-2-propen-1-one; MTC, 2-methoxy-5-(2,3,4-trimethoxyphenyl)-2,4,6-cycloheptatrien-1-one; TME, tropolone methyl ether; CD, circular dichroism.

0006-2960/96/0435-2008$12.00/0

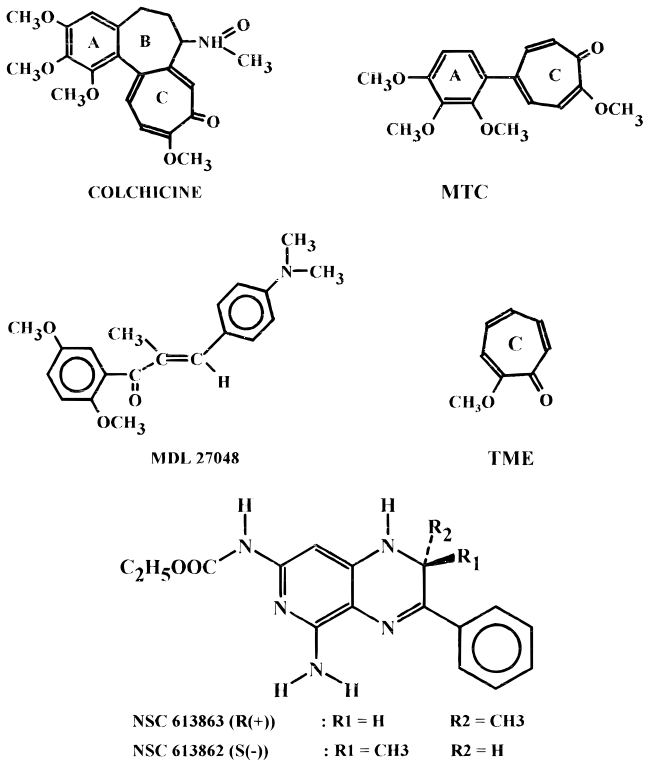

FIGURE 1: Structures of both enantiomers, MDL27048, colchicine, and analogs.

Among the 1,2-dihydro-3-phenylpyrido[3,4-*b*]pyrazin-7-yl carbamates, NSC 370147 ethyl 5-amino-1,2-dihydro-2-methyl-3-phenylpyrido[3,4-*b*]pyrazin-7-yl carbamate is an antimitotic drug (Wheeler *et al*., 1981) which can competitively inhibit the binding of tritium-labeled colchicine (Bowdon *et al*., 1987). Moreover, NSC 370147 is a racemic compound; its two enantiomers (Figure 1) NSC 613862 [(*S*)-(−)] (CI 980) and NSC 613863 [(R)-(+)] have been isolated (Temple & Rener, 1989). They displayed significant differences in potency in several biological activities. In fact, recent work on tubulin polymerization in vitro and on cell proliferation proved that the S-isomer is the more potent inhibitor (De Ines *et al*., 1994). Both isomers bind to one high-affinity site and to several low-affinity sites on tubulin. A large increase in fluorescence is provoked by binding of the R-isomer to tubulin at the high-affinity binding site. This is not observed for the S-isomer. Moreover, equilibrium studies of their binding showed that they were displaced by podophyllotoxin and MTC and that they induced GTPase activity in tubulin (Leynadier *et al*., 1993).

To better understand the mechanism of action of these compounds and the differences in their biological activities, we have studied their binding by the fluorescence stopped-flow technique. The temperature dependence of the kinetic parameters allowed us to determine the activation thermodynamic parameters of the individual steps and the overall enthalpy changes for the R-isomer. The direct study of the kinetics of S-isomer binding was hampered by the big signal due to the low-affinity sites, as shown by the binding to the tubulin-colchicine complex. For the S-isomer, we therefore used the competition kinetics between R- and S-isomers. Dissociation of the S-isomer from the tubulin complex was studied by displacement with MTC. It was unfortunately not possible to fully describe the S-isomer kinetic pathway. Finally, we compared the reaction paths of the R-isomer with those of colchicine, MTC, and MDL 27048.

MATERIALS AND METHODS

Protein Purification. Tubulin was purified from bovine and porcine brain by two different methods.

Method 1. Microtubule protein was purified from pig brain homogenate by two cycles of temperature-dependent assembly/disassembly according to the method of Shelansky *et al*. (1973) modified as previously described (Engelborghs *et al*., 1977). This preparation contained about 15% of microtubule-associated proteins (MAPs). Pure tubulin was obtained by phosphocellulose chromatography on Whatman P11 according to Weingarten *et al*. (1975) and gel filtration chromatography on Sephadex G25. The tubulin concentration was determined by two-component analysis using the absorption measured at 278 and 255 nm and the following extinction coefficients: for tubulin, 1.2 L g^{-1} cm^{-1} at 278 nm (Harrison *et al*., 1976) and 0.65 L g^{-1} cm^{-1} at 255 nm; for GTP, 12.17×10^3 and 7.66×10^3 M^{-1} cm^{-1} at 255 and 278 nm, respectively.

Method 2. Calf brain tubulin was purified by ammonium sulfate fractionation and ion-exchange chromatography, stored in liquid nitrogen, and prepared for use as described by Lee *et al*. (1973) and Andreu *et al*. (1984). The protein concentrations were determined spectrophotometrically with extinction coefficients of $\epsilon_{275nm} = 1.07$ L g^{-1} cm^{-1} (0.5% sodium dodecyl sulfate in aqueous buffer) and $\epsilon_{275nm} = 1.09$ L g^{-1} cm^{-1} (6 M guanidine hydrochloride) as reported (Weisenberg *et al*., 1968; Lee *et al*., 1973; Andreu *et al*., 1984).

Preparation and Isolation of the Tubulin−Colchicine Complex. The tubulin−colchicine complex was prepared by incubating the tubulin at 37 °C for 30 min with 1 mM colchicine. Isolating the tubulin−colchicine complex from the free ligand by passing it through a Sephadex G25 column showed a stoichiometry of one colchicine per tubulin dimer. The concentration of the tubulin−colchicine complex was determined spectrophotometrically with extinction coefficients of $\epsilon_{278nm} = 1.2$ L g^{-1} cm^{-1} for tubulin and $\epsilon_{350nm} = 16\,600$ M^{-1} cm^{-1} for colchicine.

Chemicals. NSC 613863 (R)-(+) and NSC 613862 (S)-(−) (CI 980) were synthesized as described by Temple and Rener (1989). Stock solutions were made in dimethyl sulfoxide and stored at −20 °C. Concentrations were measured spectrophotometrically with the extinction coefficient values $\epsilon_{374nm} = 15\,400$ M^{-1} cm^{-1} for R and 15 100 M^{-1} cm^{-1} for S (Temple & Rener, 1989). MTC [2-methoxy-5-(2,3,4-trimethoxyphenyl)-2,4,6-cycloheptatrien-1-one] was a gift from Dr J. Fitzgerald; its concentration was determined spectrophotometrically using $\epsilon_{343nm} = 17\,600$ M^{-1} cm^{-1} (Andreu *et al*., 1984). Colchicine was from Aldrich Chemical Co.; an extinction coefficient of $\epsilon_{350nm} = 16\,600$ M^{-1} cm^{-1} was used to determine its concentration. TME (tropolone methyl ether) was a gift from Dr J. Fitzgerald; its concentration was determined spectrometrically using an extinction coefficient at 236 nm of $\epsilon_{236nm} = 25\,900$ M^{-1} cm^{-1}. All kinetic measurements were done in a buffer consisting of 50 mM MES, 70 mM NaCl, 1 mM $MgCl_2$, 1 mM EGTA, 1 mM NaN_3, adjusted to pH = 6.4 with NaOH. $CaCl_2$ was added to a final concentration of 1 mM to prevent assembly. The percentage of DMSO was maintained at 5% (v/v) to keep the R and S compounds soluble (as in the case of the appropriate blanks).

Kinetic Association Experiments. Association kinetics were measured in a stopped-flow apparatus described elsewhere (Lambeir & Engelborghs, 1981). Excitation was done at 380 nm, and emission was collected through a Kodak Wratten filter (cutoff at 440 nm). The dead time of the instrument was determined with the reaction of *N*-bromosuccinimide with *N*-acetyltryptophanamide (Peterman, 1979) and was about 1.5 ms. The kinetic curves were analyzed for multiple exponentials by nonlinear least-squares fitting based on the Marquardt algorithm (Bevington, 1969).

Dissociation Kinetics Experiments. The kinetics of the dissociation reaction of the R-isomer were determined in the stopped-flow apparatus described above. The kinetics of the dissociation reaction of the S-isomer were determined in a Kontron SFM25 spectrofluorimeter with 1 cm × 1 cm thermostated cells (Hellma). The excitation and emission wavelengths used were 400 and 460 nm, respectively. Slit widths were 5 nm for excitation and emission. The data were acquired directly by a personal computer. Data files were imported into a commercial graphics/curve-fitting program (Sigmaplot) and fitted via a nonlinear least-squares procedure.

Competition Experiments with TME. TME competition experiments were done with a Kontron SFM25 spectrofluorimeter with 1 cm × 1 cm thermostated cells (Hellma). The excitation wavelength used was 420 nm in order to minimize the inner filter effect due to the absorption of TME, and the emission wavelength was 460 nm. Slit widths were 5 nm for excitation and emission. Tubulin was incubated with various amount of TME (from 0 to 10 mM) for 30 min at 25 °C. Then R- or S-isomers were added to reach 2 μM and the fluorescence signal was monitored. The percentage of inhibition of R- and S-isomer binding in presence of TME was calculated using their binding in the absence of TME as reference. For the R-isomer, the same experiments were also performed in the stopped-flow apparatus.

RESULTS

R-Isomer Association Kinetics. The structure of the different molecules involved in this study is represented in Figure 1. Figure 2A shows the time course of the increase in the fluorescence of R-isomer when binding to tubulin. Analysis of the data with a sum of two exponentials gives a much smaller residual least-squares sum and a better spreading of the residuals than with one exponential (see Figure 2B).

$$F = F_\infty - \Delta F_1 \exp(-k_{obs1}t) - \Delta F_2 \exp(-k_{obs2}t)$$

where F_∞ is the fluorescence at infinite time and ΔF_1, k_{obs1}, ΔF_2, and k_{obs2} are the amplitudes and the observed rate constants of the first and second phases, respectively.

Figure 3A,B shows the concentration dependence of the observed rate constants for the two phases at several temperatures. The rate constants at [R] = 0 were obtained from displacement experiments (see below). Taking these intercepts into account, the first observed rate constant (k_{obs1}) shows a linear concentration dependence whereas the second rate constant (k_{obs2}) displays a pronounced deviation from the linear relation expected for a simple pseudo-first-order concentration dependence.

Taking into account the apparent overall association equilibrium constants established for the R-enantiomer

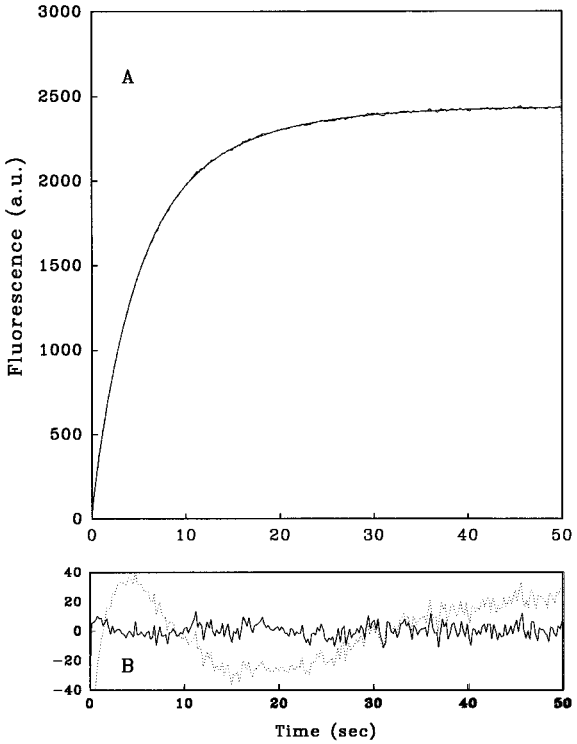

FIGURE 2: A. Fluorescence increase upon the binding of the R-isomer (23 μM) to tubulin (5 μM) observed in a stopped-flow experiment at 25 °C. The experimental curve was fitted with a sum of two exponentials. The calculated rate constants are $k_{obs1} = 0.28 \pm 0.02$ s^{-1} and $k_{obs2} = 0.113 \pm 0.006$ s^{-1}. B. The residuals (experimental curve − calculated curve) for the R-isomer are shown for argument's sake. The full line represents the residuals for a two-exponential fit, the dotted line for a single-exponential fit.

(Leynadier *et al*., 1993), we suggest the following two-step mechanism similar to that of colchicine binding (Garland, 1978): a fast initial binding followed by a slow conformational change

$$T + R \underset{k_{-1}}{\overset{k_1}{\rightleftharpoons}} TR \underset{k_{-2}}{\overset{k_2}{\rightleftharpoons}} TR^*$$

where k_1, k_2, k_{-1}, and k_{-2} are the forward and the backward rate constants of the first and second steps, respectively. The difference with the observation of Garland (1978) is that the first step can be seen separately because it is sufficiently slow and it is accompanied by a change of the fluorescence of the R-isomer. Here, the first phase corresponds to the initial binding T + R ⇌ TR, which gives in pseudo-first-order conditions $k_{obs1} = k_1[R] + k_{-1}$. The second phase can be described as follows: $k_{obs2} = k_{-2} + k_2K_1[R]/(1 + K_1[R])$ with $K_1 = k_1/k_{-1}$. The fact that the value of K_1 determined by the data of Figure 3B corresponds to k_1/k_{-1} determined in Figure 3A supports the model proposed.

R-Isomer Dissociation Kinetics. The dissociation rate constants were determined independently by displacement experiments in which an excess of MTC was added to a preformed complex of tubulin and R-enantiomer. The bound isomer is replaced by MTC (Leynadier *et al*., 1993). When the overall association rate constant of MTC ((K_1k_{2MTC})-[MTC]) is much larger than the overall association rate constant of R ($(K_1k_2)_R$[R]), every dissociating molecule of R is replaced by a molecule of MTC and the dissociation rate constant of R is the rate-limiting step (it therefore does not matter whether the fluorescence signal is coming from

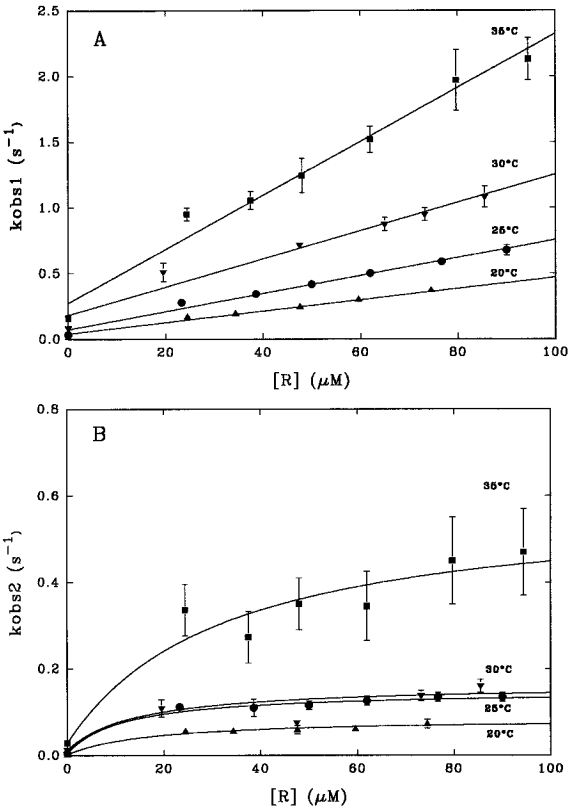

FIGURE 3: A. Concentration dependence of the largest observed rate constant (k_{obs1}) for the binding of R-isomer to tubulin, at different temperatures. The rate constant at [R] = 0 was obtained from the displacement experiments with MTC (see Figure 4). The continuous line is the linear fitting to the equation. $k_{obs1} = k_1[R] + k_{-1}$. Each point represents the mean result of ten measurements. B. Concentration dependence of the smallest observed rate constant (k_{obs2}) corresponding to the second phase of the reaction. The rate at [R] = 0 was also obtained from the displacement experiments. Each point represents the mean of ten experiments. The solid lines represent the best fit to the equation $k_{obs2} = k_{-2} + k_2K_1[R]/(1 + K_1[R])$.

the increase in MTC fluorescence or from the decrease in R fluorescence). In our conditions at 25 °C

$$(K_1k_2)_{MTC}[MTC] = 273 \times 58.5 \times 1000 \times 10^{-6} = 15.97\ s^{-1}$$

$$(K_1k_2)_R[R] = 195\ 171 \times 0.143 \times 10 \times 10^{-6} = 0.280\ s^{-1}$$

A typical fluorescence curve for the displacement of the R-enantiomer is depicted in Figure 4A. The dissociation of the tubulin−R complex was found to be well described by two exponentials (see Figure 4B) giving rise to the rate constants k_{-1} and k_{-2}.

The determination of the binding kinetics at different temperatures allowed the activation energies of the R-isomer to be calculated at each step (Ea_1 and Ea_2). The activation energies Ea_{-1} and Ea_{-2} in the dissociation direction were obtained from the displacement experiments at different temperatures (see Table 1).

S-Isomer Association Kinetics. For the S-enantiomer, it has been shown (Leynadier *et al*., 1993; Figure 5) that the fluorescence increase resulting from the binding of the S-isomer to tubulin is only slightly higher than that of its binding to tubulin−colchicine, on which the low-affinity sites

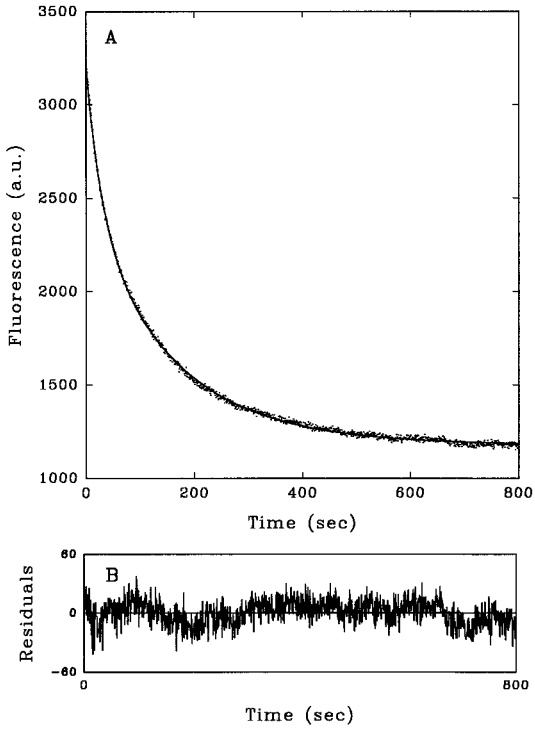

FIGURE 4: A. Displacement of the R-isomer (10 μM) bound to tubulin (5 μM) by an excess of MTC (1 mM) at 25 °C. The fluorescence decrease was fitted with a sum of two exponentials. The observed rate constants were $k_{obs1} = 0.035 \pm 0.007\ s^{-1}$ and $k_{obs2} = 0.0055 \pm 0.0006\ s^{-1}$. B. The residuals for the fitting with two exponetials.

Table 1: Thermodynamic and Kinetic Parameters of the Binding of the R-Isomer to Tubulin[a]

	R
k_1 ($M^{-1}\ s^{-1}$)	6831 ± 367
Ea_1 (kJ mol^{-1})	81 ± 6
k_{-1} (s^{-1})	0.035 ± 0.007
Ea_{-1} (kJ mol^{-1})	114 ± 17
k_2 (s^{-1})	0.143 ± 0.008
Ea_2 (kJ mol^{-1})	86 ± 25
k_{-2} (s^{-1})	$(5.5 \pm 0.6) \times 10^{-3}$
Ea_{-2} (kJ mol^{-1})	137 ± 5

[a] Individual rate constants are given at 25 °C; activation parameters for each rate constant were obtained from the temperature dependence of these rate constants (see Figures 3 and 4).

are still accessible. Kinetic studies with the tubulin−colchicine complex showed a large signal which can be fitted by the sum of two exponentials (Figure 5). The observed rate constants obtained for the first amplitude (see Table 2) are fitted by a straight line, giving the association rate constant $k_+ = (2.6 \pm 1.0) \times 10^4\ M^{-1}\ s^{-1}$ and the dissociation rate constant $k_- = 18 \pm 5\ s^{-1}$. The overall affinity constant $K_a = k_+/k_-$ was $1.5 \times 10^3\ M^{-1}$. This value is in agreement with the one found by a direct determination using the Hummel and Dreyer gel permeation technique (Leynadier *et al*., 1993). A similar fitting of the observed rate constants for the second phase gave about the same values, suggesting the presence of other low-affinity sites. The observed rate constants obtained with unliganded tubulin were very similar to those obtained with the tubulin−colchicine complex, indicating that one cannot obtain information about the high-affinity site in this way. We therefore used competition kinetics between R- and S-isomers to determine the kinetic parameters of S-binding. In the stopped-flow apparatus,

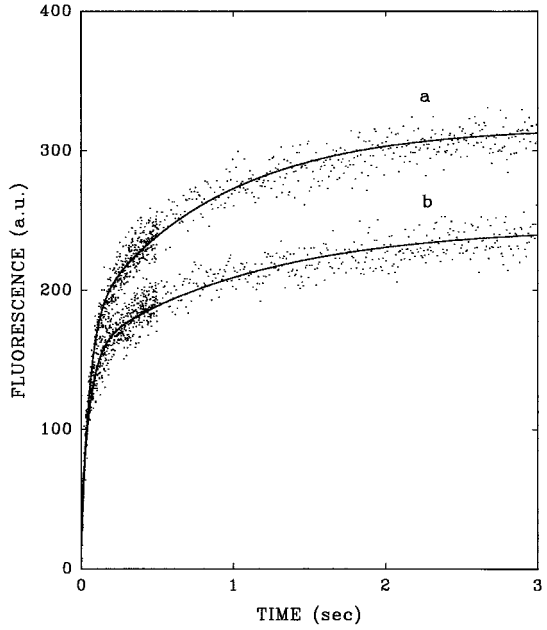

FIGURE 5: Time course of fluorescence increase upon binding of 27 μM S-isomer to 5 μM tubulin (trace a) and to 5 μM tubulin−colchicine complex (trace b) at 25 °C. The signals are fitted with a sum of two exponentials. Experimental (•••) and fitted (—) curves are shown. Values of k_{obs1} (17.7 ± 1 s^{-1}) and k_{obs2} (1.09 ± 0.07 s^{-1}) were obtained for the association of the S-isomer to tubulin, and the same values (k_{obs1} = 18 ± 1 s^{-1} and k_{obs2} = 0.95 ± 0.05 s^{-1}) were obtained for the tubulin−colchicine complex.

Table 2: Association Kinetics of the S-Isomer to the Tubulin−Colchicine Complex (5 μM) at 25 °C

[S] (μM)	first amplitude	k_{obs1} (s^{-1})	second amplitude	k_{obs2} (s^{-1})
27	117 ± 5	18 ± 1	90 ± 7	0.95 ± 0.05
34	126 ± 10	18.9 ± 1	105 ± 9	0.96 ± 0.20
51	109 ± 6	19.2 ± 1	90 ± 7	1.05 ± 0.06
75	120 ± 6	19.5 ± 1	107 ± 7	1.1 ± 0.08

tubulin was mixed with a solution containing both R-isomers (10 μM) and S-isomers (various concentrations). Only the R-isomer contributed significantly to the amplitude of the signal (the quantum yield of R-isomer−tubulin complex was much higher than that of the S-isomer−tubulin complex). In Figure 6A, trace a shows the binding of the R-isomer to tubulin and the trace b represents the binding of the R-isomer together with the S-isomer to tubulin. The curves were again fitted with a sum of two exponentials. As shown in Figure 6B, the observed rate constants increased linearly with the concentrations of S-isomer. That competition between a reporter molecule (R) and a second molecule that does not give a measurable signal (S) leads to the increase in the observed rate constant of the reporter binding has been shown before (Engelborghs & Fitzgerald, 1987). This is analogous to the determination of the rate constant of a radioactive-labeled molecule where the signal comes only from the radioactive molecules, while all the molecules (radioactive + nonradioactive) determine the observed rate constant. The slopes give the rate constants for the association of the S-isomer to tubulin; the fast rate constant value was 19 500 ± 300 M^{-1} s^{-1}, and the slow rate constant was 10 000 ± 1 200 M^{-1} s^{-1}.

S-Isomer Dissociation Kinetics. The dissociation rate constant was determined by displacement experiments, where an excess of MTC was added to a preformed complex of tubulin and S-isomer. As described above for the R-isomer,

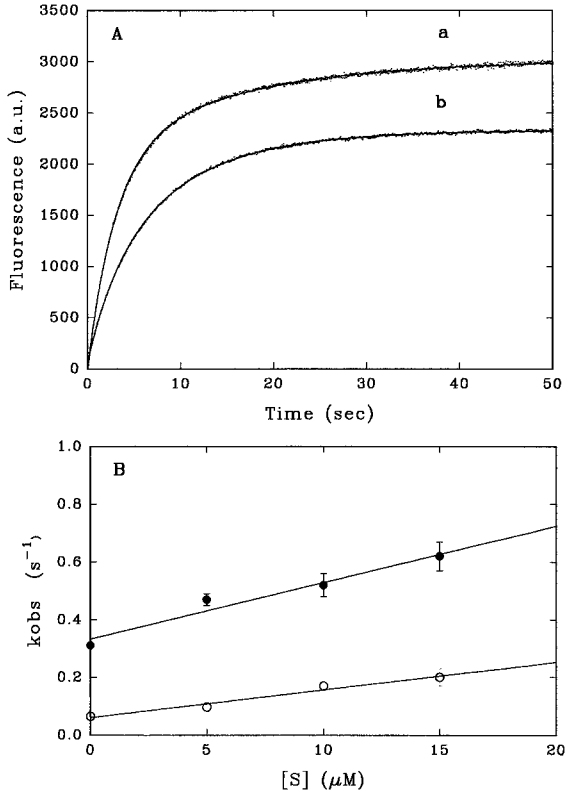

FIGURE 6: Competition kinetic experiments for R- and S-isomer binding to tubulin. A. Time course of fluorescence increase upon binding of 10 μM R-isomer to 5 μM tubulin (trace a). Trace b shows binding of 10 μM R-isomer together with 15 μM S-isomer to 5 μM tubulin. Experiments were performed at 25 °C. Experimental and fitted curves are shown. In these conditions the signal was fitted with a sum of two exponentials. B. In the stopped-flow apparatus, 5 μM tubulin was mixed with a solution of 10 μM R-isomer containing increasing concentrations of S-isomer. Both observed rate constants increased linearly with the concentrations of S-isomer. The slopes gave the association rate constants k_{+fast} = 19 500 ± 300 M^{-1} s^{-1} and k_{+slow} = 10 000 ± 1 200 M^{-1} s^{-1} for the two phases.

every dissociating molecule of S-isomer will be replaced by a molecule of MTC when the overall association rate of MTC binding (K_1k_2[MTC] = 273 × 58.5 × 200 × 10^{-6} = 3.19 s^{-1}) is much larger than the overall association rate of the S-isomer (k_+[S] = 19 500 × 2 × 10^{-6} = 0.039 s^{-1}). Figure 7 shows the dissociation of the S-isomer−tubulin complex. The fluorescence decrease was monitored by a classical spectrofluorimeter, and the curve was fitted with a single exponential (k_- = 1.2 × 10^{-3} s^{-1}). The total fluorescence decrease amounted to about 23% of the initial fluorescence, indicating that only a limited fraction of bound S-isomer can be displaced by MTC. This residual fluorescence signal may be due to the binding of the S-isomer to the low-affinity binding sites. The quantum yield of the fluorescence of the binding of S-isomer to these lower affinity sites is larger than that of the binding of S to the high-affinity (specific) site [see Figure 5 in Leynadier *et al*. (1993)]. The temperature dependence study allowed us to calculate the activation energy for the dissociation step: 168 ± 4 kJ mol^{-1}.

Effects of TME. Preliminary results obtained using tropolone methyl ether as a blocking agent of the ring C subsite indicated an inhibition of R- and S-isomer binding (Leynadier *et al*., 1993). To obtain more precise results, we performed kinetic experiments in the presence of TME. The kinetics of R-isomer binding were studied at 20 μM R-isomer

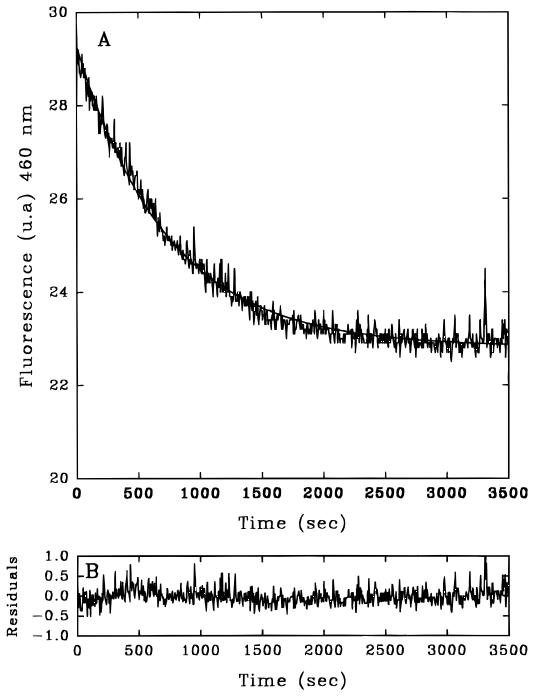

FIGURE 7: A. Displacement kinetics of the S-isomer bound by MTC at 25 °C. In the spectrofluorimeter, a tubulin solution of 1 μM was mixed with 2 μM S-isomer; when equilibrium was reached, 200 μM MTC was added and the data were collected. The curve was fitted with one exponential, and a k_{obs} value of 0.0012 ± 0.0002 s^{-1} was found. Excitation was done at 400 nm, and emission was measured at 460 nm; 5 nm slits were used. B. The residuals for the fitting with one exponential.

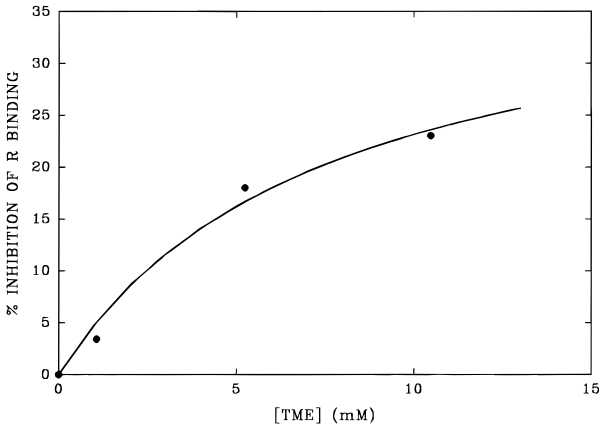

FIGURE 8: Relative inhibition (reduction of the fluorescence signal) of the R-isomer binding in presence of increasing concentrations of TME at 25 °C. A binding constant for TME was calculated by fitting the curve to a binding hyperbola. The binding constant was 135 ± 100 M^{-1} at 25 °C.

and 5 μM tubulin preincubated for 30 min at 25 °C with various millimolar concentrations of TME. The amplitude of the signal was found to be decreased relative to the reaction in absence of TME but the rate constants were not influenced. Again, we could not conduct similar experiments with the S-isomer in the stopped-flow apparatus. Therefore, the variation of the amplitude of the S-isomer signal was measured with a Kontron spectrofluorimeter (see Materials and Method). As for the R-isomer, the amplitude of the S-isomer signal was decreased in presence of TME. As shown in Figure 8 the percentage of the decrease in bound R-enantiomer can be fitted with a binding hyperbola. On the basis of these calculations, the equilibrium binding constant of TME was 135 ± 100 M^{-1}. This value is in agreement with the value determined recently by Engelborghs *et al*. (1993), 60−95 M^{-1}.

DISCUSSION

Equilibrium methods have provided massive quantities of information on the binding of colchicine and its analogs. Kinetic studies have been performed on several of them: colchicine (Garland, 1978; Lambeir & Engelborghs, 1981), C_7-substituted colchicinoid (Pyles & Hastie, 1993), MTC (Engelborghs & Fitzgerald, 1986, 1987), and MDL (Silence *et al*., 1992). The first three are structural analogs of colchicine. In this paper, we have studied the kinetics of binding of the R- and S-enantiomers, which have no structural resemblance to colchicine site ligands.

The overall binding constant [(5.1 ± 2.1) × 10^6 M^{-1}] calculated (K_1K_2) at 25 °C with the R-isomer in this study agrees fairly well with the value (2.7 × 10^6 M^{-1}) measured by equilibrium ligand fluorescence (Leynadier *et al*., 1993). However, for the S-isomer, in this study at 25 °C, the overall binding constant was 4−5 times higher than the equilibrium binding contant measured by ligand fluorescence titration. This discrepancy can probably be attributed to the indirect way of determining the association kinetics of the S-enantiomer and probably to the difficulty in determining the binding constant of the specific sites in the presence of low-affinity sites giving large fluorescence signals.

The kinetic behavior of the R-enantiomer is formally analogous to that of colchicine, MTC, and MDL27048. Indeed, the concentration dependence of the two observed rate constants can also be explained by a two-step mechanism: an initial equilibrium binding followed by a slow second step. However, the most interesting difference between the kinetic behaviors of R-isomer and colchicine is that the first step of the R binding is sufficiently slow and accompanied by a change of the fluorescence of R. The individual rate constants could thereby be determined. For colchicine and MTC, the second step is allocated to tubulin and is accompanied by a change in the protein far-UV circular dichroism and by the appearance of GTPase activity (Andreu & Timasheff, 1982). The binding of the R-isomer induces GTPase activity (Leynadier *et al*., 1993). This finding indicates that, as for colchicine, the second step includes a conformational change of tubulin. However, MDL 27048 does not lead to CD changes of tubulin and does not induce GPTase activity (Peyrot *et al*., 1992). The second step of MDL 27048 binding must represent a smaller conformational change of tubulin or a deformation of only the drug. Indeed, ring deformation cannot be ruled out, because a detailed CD spectroscopic study of the two enantiomers indicated that they exhibit large perturbation upon binding to tubulin (paper in preparation, V. Peyrot).

For the R-enantiomer, in pseudo-first-order conditions, only the slow phase exhibited a nonlinear concentration dependence. For colchicine, MTC, and MDL 27048 both phases show a highly pronounced deviation from the linear relation expected (Garland, 1978; Lambeir & Engelborghs, 1981; Engelborghs & Fitzgerald, 1986, 1987; Silence *et al*., 1992). The two phases have been attributed to the binding to different isoforms (or classes of isoforms) of tubulin (Banerjee & Luduena, 1987, 1991, 1992). Thus, in the concentration range used in this work, the R-enantiomer may

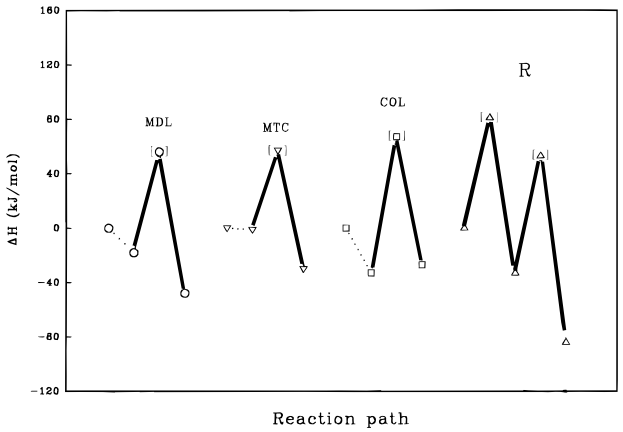

FIGURE 9: Reaction path for the binding of MDL 27048, MTC, colchicine, and the R-enantiomer to tubulin: (○) MDL 27048; (▽) MTC; (□) colchicine; (△) R. For MDL, MTC, and colchicine, the fast isoform is represented. Dotted lines are used to represent initial binding because the activation barriers are unknown. The transition states are designated with the square parentheses ([ ]).

be unable to distinguish between different isoforms (or class of isoforms) of tubulin. For the S-isomer, the competition experiments with R-isomer allowed us to determine the overall kinetic association constant. Simulation experiments taking into account the two-step binding of R-isomer and a one-step binding of the S-isomer (the less complicated model) showed a linear variation of the two observed rate constants versus S-isomer concentrations, in agreement with the competition experiments (see Figure 6B). The slope obtained for the fast phase represents the overall association rate constant, k_+, for the S-isomer. The slope for the slow phase also represents k_+ but also includes a mixture of the equilibrium and kinetic constants of both enantiomers, which lowers the k_+ value. At this stage, no more information can be obtained on the mechanism of S-isomer binding. However, it appears that, like its isomer, the S-enantiomer cannot distinguish between the two different tubulin isoforms.

The kinetic pathways of the binding of MTC, MDL 27048, colchicine, and the R-enantiomer are illustrated in Figure 9. The first reaction is exothermic for colchicine, MDL, and the R-isomer but is nearly athermic for MTC binding to tubulin. For the first time and only for the R-isomer, the activation barrier of this first reaction step (Ea_1) has been measured. The difference in the activation energy for k_1 between the R-isomer and MTC, MDL 27048, and colchicine can therefore be attributed to a steric effect from the protein for entrance and exit from the initial state or/and a contribution for deformation of the R-isomer in both ways. This means that the R-isomer−tubulin initial complex needs to be largely deformed or repositioned to enter the final state. Diaz and Andreu (1991) reported that the activation energy, Ea_2, of colchicine binding is about twice that of MTC binding. They attributed this to the presence of ring B, which is absent in MTC and may constitute a transient kinetic impediment to binding. For the S-enantiomer, the activation energy for the dissociation step (168 ± 4 kJ mol^{-1}) was higher than that of the R-enantiomer (137 ± 8 kJ mol^{-1}), indicating that the position of the methyl group has an influence on this transition. For colchicine and MTC, the different steps have been attributed to different constituent rings, although opinions differ (Andreu *et al*., 1991; Engelborghs *et al*., 1993), while the middle ring essentially influences only the kinetic barrier for the second step (Pyles & Hastie, 1993). Here the situation seems clearer, and the position of the methyl group seems to create a very high energy barrier for the second step.

The inhibition of the binding of R- and S-isomer to tubulin by excess of MTC in an equilibrium study (Leynadier *et al*., 1993) and the displacement experiments in this work show that subsite A of colchicine was implicated in the binding of both enantiomers. The competition experiments with the colchicine ring C analog, TME, demonstrated that subsite C is also involved in the interaction of these molecules with tubulin.

Cellular studies of the effects of both enantiomers have been performed (De Ines *et al*., 1994). However, the reassembly of the cytoplasmic microtubules of PtK2 cells after removal of the S- and R-enantiomers is considerably slower than with MTC or nocodazole but similar to that of colchicine. For colchicine, this slow reversibility may be linked with the very slow dissociation rate constant of binding to tubulin. For both enantiomers, the values of the dissociation rate constant are not consistent with the slow reassembly of microtubules.

We can now make the following conclusions:

(1) The R-enantiomer binds to tubulin in two steps: an initial binding followed by a conformational change.

(2) As with colchicine and its analog MTC, the binding kinetics of the R-isomer are biphasic, but these two phases cannot be attributed to the presence of two different isoforms of tubulin. We attributed them to a sequential process.

(3) For the R-isomer, the entire thermodynamic pathway has been determined.

(4) For the S-isomer, the results do not provide enough information to solve all the details of its mechanism of binding to tubulin.

(5) The activation energy for the dissociation step is larger for tubulin−S-isomer than for tubulin−R-isomer due to the position of the methyl group.

ACKNOWLEDGMENT

We are grateful to Dr. M. Sarrazin for helpful discussions and for his assistance with computer-collected data. We thank Dr. T. J. Fitzgerald for the gift of MTC and TME.

REFERENCES

Andreu, J. M., & Timasheff, S. N. (1982) *Biochemistry 21*, 6465−6476.

Andreu, J. M., & Timasheff, S. N. (1982) *Biochemistry 21*, 534−543.

Andreu, J. M., Gorbunoff, M. J., Lee, J. C., & Timasheff, S. N. (1984) *Biochemistry 23*, 1742−1752.

Andreu, J. M., Gorbunoff, M. J., Medrano, F. J., Rossi, M., & Timasheff, S. N. (1991) *Biochemistry 30*, 3777−3786.

Banerjee, A., & Luduena, R. F. (1987) *FEBS Lett. 219*, 103−107.

Banerjee, A., & Luduena, R. F. (1991) *J. Biol. Chem. 266*, 1689−1691.

Banerjee, A., & Luduena, R. F. (1992) *J. Biol. Chem. 267*, 13335−13339.

Bevington, P. R. (1969) *Data Reduction and Error Analysis for the Physical Sciences*, pp 235−240, McGraw-Hill, New York.

Bowdon, J. B., Waud, W. R., Wheeler, G. P., Hain, R., Dansby, L., & Temple, C., Jr. (1987) *Cancer Res. 47*, 1621−1626.

De Ines, C., Leynadier, D., Barasoain, I., Peyrot, V., Garcia, P., Briand, C., Gregory, A., Rener, G., & Temple, C., Jr. (1994) *Cancer Res. 54*, 75−80.

Diaz, J. F., & Andreu, J. M. (1991) *J. Biol. Chem. 266*, 2890−2896.

Dustin, P. (1978) *Microtubules*, Springer-Verlag, Berlin.

Engelborghs, Y., & Fitzgerald, T. J. (1986) *Ann. N. Y. Acad. Sci. 466*, 709−717.
Engelborghs, Y., & Fitzgerald, T. J. (1987) *J. Biol. Chem. 262*, 5204−5209.
Engelborghs, Y., De Maeyer, L. C. M., & Overbergh, N. (1977) *FEBS Lett. 80*, 81−85.
Engelborghs, Y., Dumortier, C., D'Hoore, A., Vandecandelaere, A., & Fitzgerald, T. J. (1993) *J. Biol. Chem. 268*, 107−112.
Fitzgerald, T. J. (1976) *Biochem. Pharmacol. 25*, 1383−1387.
Garland, D. L. (1978) *Biochemistry 17*, 4266−4272.
Harrisson, C. M. H., Page, B. M., & Keir, H. M. (1976) *Nature 260*, 470−476.
Lambeir, A., & Engelborghs, Y. (1981) *J. Biol. Chem. 256*, 3279−3282.
Lee, J. C., Frigon, R. P., & Timasheff, S. N. (1973) *J. Biol. Chem. 248*, 7253−7262.
Leynadier, D., Peyrot, V., Sarrazin, M., Briand, C., Andreu, J. M., Rener, G. A., & Temple, C., Jr. (1993) *Biochemistry 32*, 10675−10682.
Luduena, R. F., Shooter, E. M., & Wilson, L. (1977) *J. Biol. Chem. 252*, 7006−7014.
Olmsted, J. B., & Borisy, G. G. (1973) *Annu. Rev. Biochem. 42*, 507−540.
Perterman, B. F. (1979) *Anal. Biochem. 93*, 442−444.
Peyrot, V., Leynadier, D., Sarrazin, M., Briand, C., Menendez, A., Laynez, J., & Andreu, J. M. (1992) *Biochemistry 31*, 11125−11132.
Pyles, E., & Hastie, S. B. (1993) *Biochemistry 32*, 2329−2336.
Shelanski, M. L., Gaskin, F., & Cantor, C. R. (1973) *Proc. Natl. Acad. Sci. U.S.A. 70*, 765−768.
Silence, K., D'Hoore, A., Engelborghs, Y., Peyrot, V., & Briand, C. (1992) *Biochemistry 31*, 11133−11137.
Temple, C., Jr., & Rener, G. A. (1989) *J. Med. Chem. 32*, 2089−2092.
Weingarten, M. D., Lockwood, A. H., Hwo, S. Y., & Kirschner, M. W. (1975) *Proc. Natl. Acad. Sci. U.S.A. 72*, 1858−1862.
Weisenberg, R. G., Borisy, G. G., & Taylor, E. (1968) *Biochemistry 7*, 4466−4479.
Wheeler, G. P., Bowdon, B. J., Werline, J. A., & Temple, C., Jr. (1981) *Biochem. Pharmacol. 30*, 2381−2384.

BI951987Y